THE PARALLEL KALMAN FILTER: AN EFFICIENT TOOL TO DEAL WITH REAL-TIME NON CENTRAL χ NOISE CORRECTION OF HARDI DATA

V. Brion⋆*, *O. Riff*⋆*, *M. Descoteaux*†*, *J.-F. Mangin*⋆*, *D. Le Bihan*⋆*, *C. Poupon*⋆*, *F. Poupon*⋆

⋆NeuroSpin, CEA/I2BM, Gif-sur-Yvette, France
†MOIVRE center, Université de Sherbrooke, Sherbrooke, Canada

ABSTRACT

We propose a novel real-time non central χ (nc-χ) noise correction method for diffusion-weighted MR data that are known to be particularly sensitive to noise, especially at high b-values. This technique aims to be real-time during the acquisition to get any map stemming from the Diffusion Tensor Imaging (DTI) and the High Angular Resolution Diffusion Imaging (HARDI) models corrected from nc-χ noise. The method is based on a Parallel Kalman Filter which is well adapted for non-Gaussian noise distributions, and which is as suitable for real time purposes as the standard Kalman filter (KF). The results on simulated and real HARDI data show that it outperforms the standard KF approach since non-Gaussian noise distributions are directly embedded in the process through their Gaussian mixture approximation.

***Index Terms*—** HARDI, Parallel Kalman, non central χ noise, noise correction, real-time.

1. INTRODUCTION

When dealing with real-time processes, the Kalman Filter (KF) comes to mind as a least-squares incremental solver very suitable for real-time purposes [1]. Unfortunately, the KF is restricted to processes corrupted by Gaussian noise. To overcome this limit, a Parallel Kalman Filter (PKF) was developed by [2], inspired from the KF with an extension to non-Gaussian noise filtering. In [2], the PKF is theoretically described for any non-Gaussian noise and is shown to be efficient in the field of Narrowband Interference Suppression. The PKF might also be able to offer a prospect in the context of real-time diffusion-weighted (DW) Magnetic Resonance Imaging (rt-dMRI) for the correction of the DW data.

The purpose of rt-dMRI is to perform diffusion tensor (DTI) and HARDI imaging during the acquisition [3]. This technique improves clinical protocols as it allows stopping and restarting acquisitions at any time without threatening the quality of the final data. Furthermore, inherited information stemming from DTI or HARDI such as maps of the apparent diffusion coefficient (ADC), maps of the generalized fractional anisotropy (GFA) and maps of the orientation distribution functions (ODFs) can be estimated at any step of the acquisition, thus saving time for clinicians since long post-processing tasks increasing the diagnosis duration can be avoided.

But, in rt-dMRI, as well as in dMRI with offline reconstruction, the noise present in the data greatly decreases image quality, especially when using high b-values. This noise was first decribed as being Rician, which is valid in case of a single-channel acquisition. In case of a multiple-channel acquisition with a Sum-of-squares (SoS) reconstruction, the measured magnitude of the magnetization follows a non central χ (nc-χ) distribution. But this hypothesis is only valid if there is no correlation between the receiving channels. Moreover, the noise is no longer stationary if correlation exists [4, 5]. However, recent work has shown that the nc-χ noise model can be a good approximation, when in addition, an effective number of channels and an effective noise variance are used [5]. A similar study was performed for Generalized Autocalibrating Partially Parallel Acquisition (GRAPPA) reconstructions [6]. When using the Sensitivity Encoding for Fast MRI (SENSE) algorithm, the nc-χ distribution simplifies again into a Rician distribution, which is a particular case of the nc-χ one [7].

Concerning MRI real-time noise correction, most of the offline correction techniques cannot be applied because they require to have acquired the entire data set for all diffusion directions encoded before starting the denoising. And yet, a real-time correction has to be done, by definition, after each new diffusion direction has been acquired. The algorithm chosen has also to be quite fast to perform corrected results nearly instantaneously during the exam. A real-time nc-χ noise correction method was already proposed by [8] in a compatible way with the rt-dMRI environment introduced by [3]. This method relies on a Linear Minimum Mean Square Error Estimator (LMMSE) extended to nc-χ noise [9], and whose corrected signal is then injected in a standard KF, embedded with a feedback loop to lower the smoothing effect inherent to the LMMSE. As the KF corrects for Gaussian noise only, the method in [8] assumes that the LMMSE leaves a Gaussian noise in the corrected signal injected in the KF. This hypothesis is precisely the major flaw of the technique because it is impossible to verify that the resulting noise is really Gaussian. Furthermore, it is highly sensitive to any error on the LMMSE estimation. To overcome this problem, we propose a new real-time noise correction based on the PKF, which directly embeds a non-Gaussian distribution through its Gaussian mixture representation. Thereby, we also perform here the first adaptation of the PKF to this particular real-time nc-χ noise correction issue.

2. METHODS

In our case, the PKF purpose is to simplify the nc-χ noise correction problem in a Gaussian one, using the idea that the distribution of a signal corrupted by any non-Gaussian noise can be approximated by a Gaussian mixture [4].

Figure 1 synthesizes the global method which can be summarized as follows: first, the LMMSE is applied to the measured DW signal $M(\mathbf{v}, \mathbf{o})$, at position $\mathbf{v} \in R^3$ for the orientation $\mathbf{o} \in S^2$, in order to give an estimate of the noise-free signal $\hat{S}(\mathbf{v}, \mathbf{o})$. Also, the noise standard deviation is estimated globally for the whole DW volume, using the method proposed by [10]:

$$\hat{\sigma} = \left(\sqrt{2}(n)_{\frac{1}{2}}\right)^{-1} \text{mode}\left(\langle M_{bg}(\mathbf{v})\rangle\right), \quad (1)$$

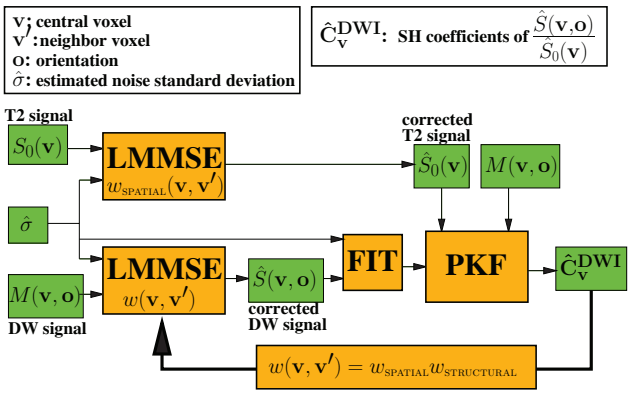


Fig. 1. The real-time noise correction algorithm in a global view.

where $M_{bg}(\mathbf{v})$ is the measured magnitude at the voxel $\mathbf{v}$ in the background region; mode ($\langle M_{bg} \rangle$) is the distribution mode of the mean of $M_{bg}(\mathbf{v})$; $(x)_n$ is the Pochhammer symbol defined as $(x)_n = \frac{\Gamma(x+1)}{\Gamma(x-n+1)}$ with Γ the Gamma function. Both estimations $\hat{\sigma}$ and $\hat{S}(\mathbf{v}, \mathbf{o})$, with the measured magnitude $M(\mathbf{v}, \mathbf{o})$ completely define the nc-χ distribution of $M(\mathbf{v}, \mathbf{o})$. This allows, in a second stage, to approximate this distribution by a Gaussian mixture using a Levenberg-Marquardt algorithm. It corresponds to the FIT block in the figure 1. Finally, this mixture of f Gaussian distributions is injected in a PKF, which calculates, in real-time, the coefficients characterizing the noise-corrected signal in the modified Spherical Harmonics (SH) basis employed in the analytical Q-ball model using a constant solid angle developed in [11].

The PKF details are given in figure 2, which shows the refinement, also called update, after the acquisition of the o^{th} diffusion orientation, of the previously corrected results of the $o-1^{th}$ diffusion orientation. The job of the PKF is to take into account each Gaussian noise through linear systems working in parallel, using the results of the approximation done by the Levenberg-Marquardt algorithm and using the vector $\mathbf{a}(o) = [A_{o1}, ..., A_{oR}]$ corresponding to the o^{th} row of the $M \times R$ matrix A of the modified SH basis, defined such that:

$$\mathbf{A} = \begin{pmatrix} Y_1(\theta_1, \phi_1) & Y_2(\theta_1, \phi_1) & \dots & Y_N(\theta_1, \phi_1) \\ \vdots & \vdots & \ddots & \vdots \\ Y_1(\theta_M, \phi_M) & Y_2(\theta_M, \phi_M) & \dots & Y_N(\theta_M, \phi_M) \end{pmatrix}, \tag{2}$$

with M the number of diffusion encoding directions, which corresponds to the number of iterations during the real-time process and $R = (N+1)(N+2)/2$ the number of Spherical Harmonics (SH) with N the maximum SH order. These linear systems (figure 2), calculated in the PKF, are then gathered in a single density being a Bayesian *a posteriori* estimate of the Gaussian mixture. This collapsed density has only one Gaussian term and can be injected in a Kalman-like filter (figure 2), which equations give the expressions of the innovation $\nu(o)$, the Kalman gain $\mathbf{k}(o)$, the normalized covariance matrix $\mathbf{P}(o)$ of the state vector $\mathbf{x}$ and the updated estimate of the state vector $\hat{\mathbf{x}}(o)$. The Kalman-like filter delivers the updated estimates of the state vectors, corresponding to the optimal corrected coefficients $\hat{\mathbf{C}}_{\mathbf{v}}^{\mathbf{DWI}}$. From them, the corrected DW signals can be obtained, as well as any map of the DTI and HARDI models.

As in [8], a feedback loop is used to limit the smoothing effect induced by the LMMSE. This loop defines weighting coefficients that are composed of a spatial and a structural term that are defined as:

$$w_{spatial}(\mathbf{v}, \mathbf{v}') = exp\left(-\frac{(\mathbf{v}'-\mathbf{v})^2}{2\alpha^2}\right), \tag{3}$$

and

$$w_{structural}(\mathbf{v}, \mathbf{v}') = exp\left(-\frac{\sum_{j=1}^{N}\left(\hat{\mathbf{C}}_{\mathbf{v}'}^{\mathbf{DWI}}(j) - \hat{\mathbf{C}}_{\mathbf{v}}^{\mathbf{DWI}}(j)\right)^2}{2\beta^2}\right), \tag{4}$$

where $\hat{\mathbf{C}}_{\mathbf{v}}^{\mathbf{DWI}}$ is the current value of the Parallel Kalman filter state vector at voxel $\mathbf{v}$ (N being the length of the state vector), and α and β are two constants driving the magnitude of the spatial and structural weightings. $w_{spatial}(\mathbf{v}, \mathbf{v}')$ modulates the influence of the neighboring voxels according to their distance from the central voxel, thus preserving resolution of thin structures. $w_{structural}(\mathbf{v}, \mathbf{v}')$ is based on a metric of Orientation Distribution Function (ODF) similarities introduced in [12] and favours neighboring voxels having a similar underlying structure. Thus, the feedback loop constrains the LMMSE spatially and structurally for better accuracy.

The PKF was initialized by setting the initial guess $\hat{\mathbf{x}}(0)$ to the null vector. The initial covariance matrix was set to $\mathbf{P}(0) = (c\mathbf{I} + \lambda\mathbf{L})^{-1}$ with $c = 10^{-6}$, as suggested by [13] to optimize the convergence of the filter. $\mathbf{I}$ represents the identity matrix, λ is a regularization factor, and $\mathbf{L}$ is the Laplace-Beltrami operator. This operator regularizes the solution and prevents remaining noise peaks to contribute to the final solution. The initial weight was defined such that: $w(\mathbf{v}, \mathbf{v}') = w_{spatial}(\mathbf{v}, \mathbf{v}')$.

To recap, this complex combination of tools (the LMMSE followed by a Levenberg-Marquardt fit to then perform the PKF) better respects the noise configuration issue than the simpler method by [8], which flaw is to assume a resulting Gaussian noise in the LMMSE corrected result injected in a KF. The next section compares both methods on the experimental front.

3. RESULTS AND DISCUSSION

We compared this new real-time method (PKF) to the one proposed by [8] on both simulated and real DW data corrupted by nc-χ noise.

3.1. Simulated DW data

We created 3D volumes of noise-free T2-weighted and DW data used as ground truth depicting a crossing of 2 fiber bundles. This simulation was done using a Gaussian mixture model for the fibre crossing, assuming that there is no water molecules' exchange between the 2 compartments corresponding to the 2 bundles. This hypothesis remains acceptable, as exchange time between compartments is much longer than the diffusion time used in dMRI experiments. To add the nc-χ noise with a number of channels $n = 4$, we first calculated the noise-free signals $S(i)$ that each channel would receive, assuming that all channels receive the same signal: $\forall i \in [\![1; n]\!], S(i) = S_{noise-free}/n$. Thus, the noisy signal is given by the non linear transform: $S_{noisy} = \left(\sum_{i=0}^{n}\left(S(i) + n_{real}(i)\right)^2 + n_{imag}(i)^2\right)^{1/2}$ where $n_{real}(i)$ and $n_{imag}(i)$ are respectively the real and imaginary noises added on

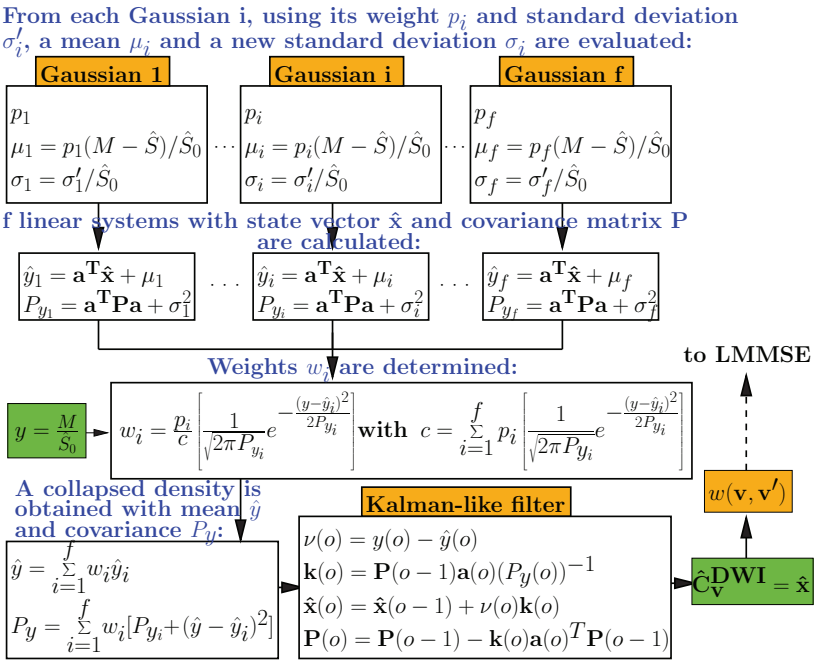


Fig. 2. The detailed PKF adapted from [2].

channel i. They are generated using a Gaussian noise distribution with different standard deviation σ going from 15 to 65 for a T2-weighted signal $S_0 = 700$.

Using a $5\times5\times5$ neighborhood, we tested the method introduced by [8] and ours on the analytical Q-ball model using a constant solid angle (CSA) developed in [11]. The maximum SH order N was set to 8 and the Laplace-Beltrami regularization factor λ was set to 0.006. To quantitatively validate our new real-time method, we measured the quadratic errors between the CSA ODFs of the noise-free data and all other data:

$$\epsilon = \sum_{\mathbf{v}=1}^{M} \left(\sum_{j=1}^{N} \left(\mathbf{C}_{\mathbf{v}}^{\mathbf{DWI}}(j) - \tilde{\mathbf{C}}_{\mathbf{v}}^{\mathbf{DWI}}(j) \right)^2 \right), \qquad (5)$$

where $\mathbf{C}_{\mathbf{v}}^{\mathbf{DWI}}$ is the SH coefficient vector of the noise-free DW signal of voxel $\mathbf{v}$ (M is the number of voxels in the field) and $\tilde{\mathbf{C}}_{\mathbf{v}}^{\mathbf{DWI}}$ is either the noisy or the corrected coefficient vector. Fig. 3 reveals a similar decreased ϵ using both methods. Nevertheless, the visual results on the CSA ODFs give a clear preference for the PKF method over the method by [8] because the crossing information in the CSA ODF is better retrieved with far less bias between the two peaks.

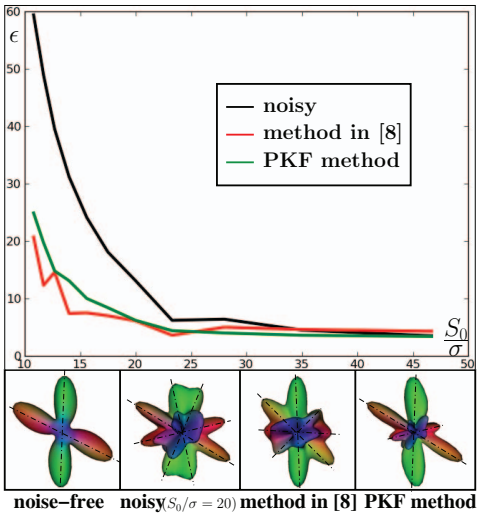


Fig. 3. Results on simulated data.

3.2. Real DW data

We also compared both real-time methods on real DW data acquired on a Magnetom Tim Trio 3T MRI system (Siemens Medical Solutions, Erlangen, Germany), using a gradient sampling scheme of 60 orientations uniformly distributed over a sphere at $b = 4500 s.mm^{-2}$. Three reference T2 weighted volumes were acquired at $b = 0 s.mm^{-2}$. The acquisition parameters were as follows: $T_E/T_R = 116ms/14s$, field of view $FOV = 198mm$, matrix 128×128, resolution $1.7 \times 1.7 \times 1.7mm^3$, GRAPPA factor of 2, read bandwidth $RBW = 1628Hz/pixel$ and a number of coils of 12 in an architecture of 4×3 coupled coils, so $n = 4$ in this case. To take into account effects from correlations between the n channels, an effective number of channels n_{eff} was calculated, as advised by [5], but we define it in an empirical manner by choosing the n_{eff} value yielding the highest SNR after correction. $n_{eff} = 2.0$ and 2.6 respectively for the PKF method and the one by [8].

We tested both methods on the DTI model (color-encoded RGB

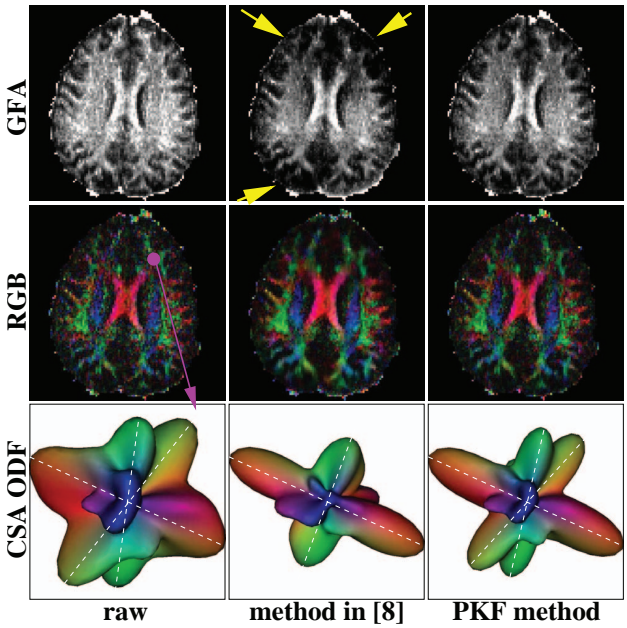


Fig. 4. Results on real data.

map) and on the analytical Q-ball model using a constant solid angle (GFA and CSA ODF maps) with $N = 8$ and $\lambda = 0.006$. Fig. 4 depicts the contrast improvement gained on the GFA and RGB maps with both methods. Some structural details (e.g. in cortical areas shown by the yellow arrows) are lost when applying the method proposed by [8], whereas they are kept with the PKF method. Also [8] produces a higher smoothing level, whereas the PKF technique provides more accuracy towards the anatomical structures which is confirmed on the ODF maps: the method in [8] neglects the raw information and loses one bundle direction. On the contrary, the CSA ODF after the PKF technique contains the expected 3 main directions and is also sharper, with a decreased bias between the peaks.

Our nc-χ noise correction was made available for real-time use, thanks to a parallelization and a distribution on a cluster of 60 CPUs that lead to a huge reduction of the processing time per volume: from 123s on a workstation to 1.5s with the cluster, thus far below the repetition time of 14s and making the technique fully compatible with real-time.

4. CONCLUSION

We developed a real-time nc-χ noise correction method, compatible with the real-time environment of [3], that does not rely on any hypothesis compared to [8], which assumes a Gaussian noise left by the LMMSE in the signal given to the KF. Moreover, our results on simulated and real data demonstrate the improvement given by our method over the one in [8]: good noise cleaning with the preservation of the details. Finally, our method is fast enough to be performed on the state-of-the-art HARDI models in real-time. To keep this possible, we assumed that the noise was stationary, as well as n_{eff}. Further work will be done to tackle the non-stationary situation.

5. REFERENCES

[1] R. E. Kalman, "A new approach to linear filtering and prediction problems," *Trans. ASME J. Basic Eng.*, vol. 82, pp. 35–45, 1960.

[2] K. N. Plataniotis, D. Androutsos, and A. N. Venetsanopoulos, "Nonlinear filtering of non-gaussian noise," *Journal Intell. Robotic Syst.*, vol. 19, pp. 207–231, 1997.

[3] C. Poupon, A. Roche, J. Dubois, J.-F. Mangin, and F. Poupon, "Real-time MR diffusion tensor and Q-ball imaging using Kalman filtering," *Med. Image Anal.*, vol. 12, pp. 527–534, 2008.

[4] C. D. Constantinides, E. Atalar, and E. R. McVeigh, "Signal-to-Noise Measurements in Magnitude Images from NMR Phased Arrays," *MRM*, vol. 38, pp. 852–857, 1997.

[5] S. Aja-Fernández and A. Tristán-Vega, "Influence of Noise Correlation in Multiple-Coil Statistical Models With Sum of Squares Reconstruction," *MRM*, vol. 67, pp. 580–585, 2011.

[6] S. Aja-Fernández, A. Tristán-Vega, and W. Scott Hoge, "Statistical noise analysis in GRAPPA using a Parametrized Noncentral Chi Approximation Model," *MRM*, vol. 65, pp. 1195–1206, 2011.

[7] O. Dietrich, J. G. Raya, S. B. Reeder, M. Ingrisch, M. F. Reiser, and S. O. Schoenberg, "Influence of multichannel combination, parallel imaging and other reconstruction techniques on MRI noise characteristics.," *Magn. Reson. Imaging*, vol. 26, pp. 754–762, 2008.

[8] V. Brion, O. Riff, J.-F. Mangin, D. LeBihan, C. Poupon, and F. Poupon, "Real-time non central Chi noise correction adapted to parallel real-time diffusion-weighted MRI: impact on real-time HARDI maps," in *Proceedings of the 28th ESMRMB*, 2011.

[9] V. Brion, C. Poupon, O. Riff, S. Aja-Fernández, A. Tristán-Vega, J.-F. Mangin, D. LeBihan, and F. Poupon, "Parallel MRI noise correction: an extension of the LMMSE to non central Chi distributions," in *Proceedings of the 14th MICCAI*, 2011.

[10] S. Aja-Fernández, A. Tristán-Vega, and C. Alberola-López, "Noise estimation in single- and multiple-coil magnetic resonance data based on statistical models," *Magn. Reson. Imaging*, vol. 27, pp. 1397–1409, 2009.

[11] I. Aganj, C. Lenglet, G. Sapiro, E. Yacoub, K. Ugurbil, and N. Harel, "Reconstruction of the orientation distribution function in single- and multiple-shell q-ball imaging within constant solid angle," *MRM*, vol. 64, pp. 554–566, 2010.

[12] Maxime Descoteaux, *High Angular Resolution Diffusion MRI: from Local Estimation to Segmentation and Tractography*, Ph.D. thesis, Université de Nice-Sophia Antipolis, 2008.

[13] R. Deriche, J. Calder, and M. Descoteaux, "Optimal Real-Time Q-Ball Imaging using Regularized Kalman Filtering with Incremental Orientation Sets," *Med. Image Anal.*, vol. 13, pp. 564–579, 2009.